Galaxy Masses as Constraints of Formation Models
Proceedings IAU Symposium No. 311, 2014
M. Cappellari & S. Courteau, eds.

doi:10.1017/S1743921315003336

The Outer Halos of Early-Type Galaxies

Ortwin Gerhard[1], Magda Arnaboldi[2] and Alessia Longobardi[1]

[1]Max-Planck-Institut für extraterrestrische Physik, Postfach 1312, Giessenbachstr. 1, 85741 Garching, Germany. email: gerhard@mpe.mpg.de, alongobardi@mpe.mpg.de
[2]European Southern Observatory, Karl-Schwarzschild-Strasse 2, D-85748 Garching, Germany. e-mail: marnabol@eso.org

Abstract. The outer halos of massive early-type galaxies (ETGs) are dark matter dominated and may have formed by accretion of smaller systems during galaxy evolution. Here a brief report is given of some recent work on the kinematics, angular momentum, and mass distributions of simulated ETG halos, and of corresponding properties of observed halos measured with planetary nebulae (PNs) as tracers. In the outermost regions of the Virgo-central galaxy M87, the PN data show that the stellar halo and the co-spatial intracluster light are distinct kinematic components.

1. Stellar and dark matter halos in simulated ETGs

Wu *et al.* (2014) studied the luminous and dark matter halos in 42 simulated early-type galaxies (ETGs) with stellar masses from $2.0\times10^{10}\mathrm{M}_\odot\ \mathrm{h}^{-1}$ to $3.4\times10^{11}\mathrm{M}_\odot\ \mathrm{h}^{-1}$. These simulated galaxies were obtained from N-body/hydrodynamical zoom re-simulations of selected halos from a dark matter cosmological simulation, including a model for star formation and feedback (Oser *et al.* 2010, 2012).

The dark matter halo density profiles of the simulated ETGs follow simple power-law models, with flat dark matter circular velocity curves (CVCs) for lower mass systems and rising CVCs for high-mass halos, corresponding to slightly falling to flat total CVCs respectively. The dark matter fractions of these systems are in the range 15-30% at the stellar half-mass radius R_e and increase to 40-65% at $5\,\mathrm{R_e}$. The short axes of simulated galaxies and their host dark matter halos are well-aligned and their (short-to-long) axis ratios are correlated.

Line-of-sight (LOS) velocity fields obtained with a time-smoothing technique out to large radii (see examples in Fig. 1) show that the rotation properties at small and large radii are correlated. Radial profiles for the cumulative specific angular momentum parameter $\lambda(R)$ are nearly flat or slightly rising, with values in $[0.06,\ 0.75]$ from $2\,\mathrm{R_e}$ to $5\,\mathrm{R_e}$. A few cases show local maxima in $|\bar{v}|/\sigma(R)$.

Many of the properties of these simulated ETGs agree remarkably well with observations of ETGs at large radii, such as briefly summarized in the next section.

2. Kinematics, angular momentum, and dark matter mass in ETG halos from PNs

Planetary nebulae (PNs) are excellent tracers for the kinematics in the faint outskirts of ETGs where kinematic measurements from integrated light are no longer possible. Various techniques have been implemented to measure radial velocities from their bright [OIII]λ5007Å line (e.g., Hui *et al.* 1995; Arnaboldi *et al.* 1998; Méndez *et al.* 2001; McNeil *et al.* 2010). With the specially built Planetary Spectrograph (PN.S) instrument (Douglas *et al.* 2002), a survey of nearby ($D < 20$ Mpc) early-type galaxy halos in the Northern hemisphere has now been completed. The new sample expands on earlier results based

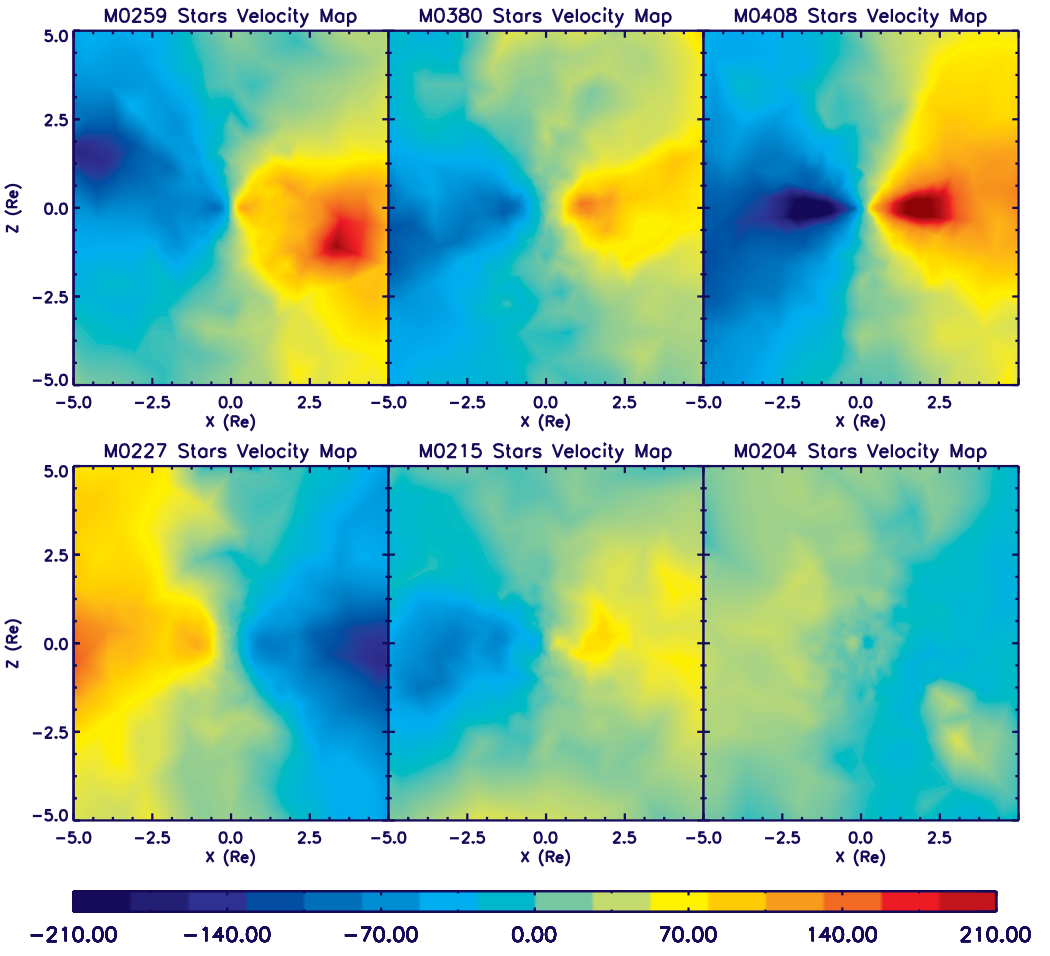

Figure 1. Edge-on mean LOS velocity maps for the stellar components of 6 selected model galaxies. The upper panels show three simulated galaxies with large scale rotation; the galaxy in the top right panel has a strong disk component from a gas rich major merger. The lower panels show three simulated galaxies with a dissipationless merging history. The galaxy in the bottom right panel shows weak major and minor axis rotation; it has a formation history with many minor mergers. From Wu *et al.* (2014).

on 6 lenticulars and 13 ellipticals (Coccato *et al.* 2009; Cortesi *et al.* 2013), to 11 S0s and 30 ellipticals with extended kinematics measured from 2-10R_e.

From the PN data one can measure the specific angular momentum out to these large radii (Fig. 2, from Cortesi *et al.* 2013) and the frequency of angular momentum misalignment between the inner region and the outer halo. One interesting, still not fully understood result is the apparent dichotomy between galaxies with quasi-Keplerian, steeply falling, velocity dispersion profiles and galaxies with nearly flat velocity dispersion profiles (Coccato *et al.* 2009). Dynamical modeling of a few of the quasi-Keplerian systems with the NMAGIC made-to-measure method (de Lorenzi *et al.* 2007) has shown a strong mass-anisotropy degeneracy (de Lorenzi *et al.* 2008, 2009), with the range of best dark matter halo profiles (Fig. 3; Morganti *et al.* 2013) consistent with those of the lower mass, simulated ETGs of Wu *et al.* (2014); see also Deason *et al.* (2012). By contrast, for massive ETGs with nearly flat dispersion profiles the inferred total CVCs are nearly

https://doi.org/10.1017/S1743921315003336 Published online by Cambridge University Press

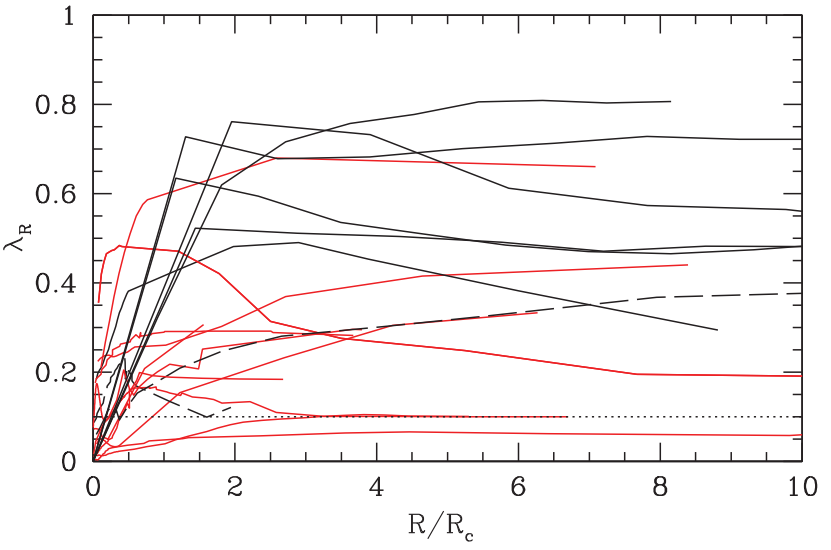

Figure 2. The λ_R parameter measuring enclosed specific angular momentum as a function of radius, for a sample of early-type galaxies. Black solid lines are S0s from Cortesi *et al.* (2013), black dashed lines are S0s from Coccato *et al.* (2009), and red lines are ellipticals from Coccato *et al.* (2009). The dotted line shows the suggested separation between slow and fast rotators (Emsellem *et al.* 2007). From Cortesi *et al.* (2013).

constant with radius (e.g., Das *et al.* 2011). Full analysis of the PN.S survey data is still on-going.

3. Distinct stellar halo and intracluster light components in the outskirts of the giant Virgo ETG M87

Brightest cluster galaxies (BCGs) have extended halos often embedded in diffuse intracluster light (ICL; e.g., Gonzalez *et al.* 2005). The ICL consists of stars moving in the cluster potential, whereas halo stars would be defined as bound to the central galaxy. However, if the BCG is located in the cluster center, it is not clear whether a clear distinction between halo and ICL is generally possible (Dolag *et al.* 2010; Cooper *et al.* 2013). An interesting case is NGC 3311 in the Hydra I cluster, where the very rapid transition of the velocity dispersion profile to cluster values suggests a continuous transition from halo to ICL (Ventimiglia *et al.* 2010).

Doherty *et al.* (2009) first investigated the transition from halo to ICL in the outermost regions of the Virgo cluster. With a small sample of PNs, they found no halo PNs beyond 150 kpc radius, and a rapidly decreasing velocity dispersion profile towards this boundary, while ICL PNs with large velocity dispersion where seen at similar radii. Based on a large sample of PN candidates indentified through on/off-band imaging (Longobardi *et al.* 2013), and kinematic follow-up with the VLT FLAMES instrument (Longobardi *et al.* 2014), it was possible to separate PNs from the M87 halo and ICL with a robust kinematic technique. Fig. 4 shows that both components coexist at similar radii with different density profiles. The relative abundance of PNs per unit bolometric luminosity and the PN luminosity function furthermore suggest that the outer M87 halo and the ICL in the Virgo core are different stellar populations.

https://doi.org/10.1017/S1743921315003336 Published online by Cambridge University Press

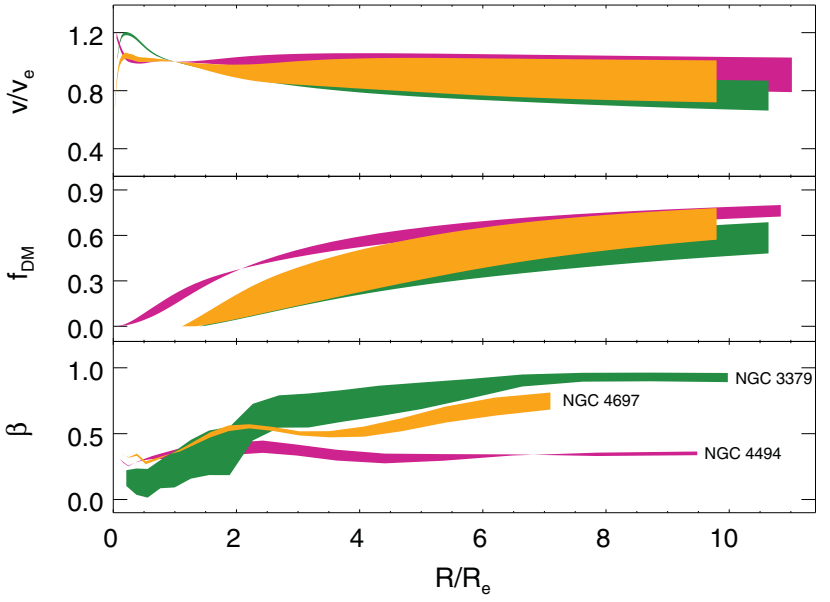

Figure 3. Radial profiles of circular velocity normalized by its value at $1R_e$ (top), dark matter fraction (middle), and anisotropy parameter (bottom), for the range of valid NMAGIC models obtained fitting the data of NGC 4494 (*violet*, Morganti *et al.* 2013), NGC 4697 (*orange*, de Lorenzi *et al.* 2008), and NGC 3379 (*green*, de Lorenzi *et al.* 2009). From Morganti *et al.* (2013).

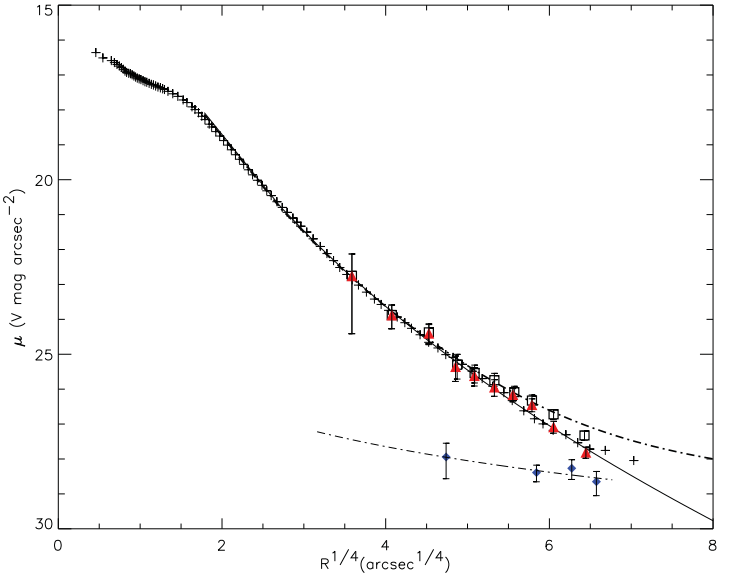

Figure 4. The logarithmic PN number density profile of the M87 halo (red triangles) and ICL PNs (blue diamonds), corrected for incompleteness as a function of the distance from the M87 centre. For comparison, the surface brightness profile from Kormendy *et al.* (2009) is shown as crosses. The ICL density decreases towards larger radii as $I_{ICL} \propto R^{-0.4}$ (dashed blue line). Black squares show the composite halo plus ICL PN number density profile, well-modelled by the two component model (dot-dashed black line, see Longobardi *et al.* (2014) for more details). Error bars account for 1 σ uncertainties from counting statistics. From Longobardi *et al.* (2014).

https://doi.org/10.1017/S1743921315003336 Published online by Cambridge University Press

References

Arnaboldi, M., *et al.* 1998, *ApJ*, 507, 759
Coccato, L., *et al.* 2009, *MNRAS*, 394, 1249
Cooper, A. P., *et al.* 2013, *MNRAS*, 434, 3348
Cortesi, A., *et al.* 2013, *MNRAS*, 432, 1010
Das, P., *et al.* 2011, *MNRAS*, 415, 1244
de Lorenzi, F., Debattista, V. P., Gerhard, O., & Sambhus, N. 2007, *MNRAS*, 376, 71
de Lorenzi, F., *et al.* 2008, *MNRAS*, 385, 1729
—. 2009, *MNRAS*, 395, 76
Deason, A. J., Belokurov, V., Evans, N. W., & McCarthy, I. G. 2012, *ApJ*, 748, 2
Doherty, M., *et al.* 2009, *A&A*, 502, 771
Dolag, K., Murante, G., & Borgani, S. 2010, *MNRAS*, 405, 1544
Douglas, N. G., *et al.* 2002, *PASP*, 114, 1234
Emsellem, E., *et al.* 2007, *MNRAS*, 379, 401
Gonzalez, A. H., Zabludoff, A. I., & Zaritsky, D. 2005, *ApJ*, 618, 195
Hui, X., Ford, H. C., Freeman, K. C., & Dopita, M. A. 1995, *ApJ*, 449, 592
Kormendy, J., Fisher, D. B., Cornell, M. E., & Bender, R. 2009, *ApJS*, 182, 216
Longobardi, A., *et al.* 2013, *A&A*, 558, A42
Longobardi, A., Arnaboldi, M., Gerhard, O., & Hanuschik, R. 2014, *A&A*, submitted
McNeil, E. K., *et al.* 2010, *A&A*, 518, A44
Méndez, R. H., *et al.* 2001, *ApJ*, 563, 135
Morganti, L., *et al.* 2013, *MNRAS*, 431, 3570
Oser, L., Naab, T., Ostriker, J. P., & Johansson, P. H. 2012, *ApJ*, 744, 63
Oser, L., *et al.* 2010, *ApJ*, 725, 2312
Ventimiglia, G., Gerhard, O., Arnaboldi, M., & Coccato, L. 2010, *A&A*, 520, L9+
Wu, X., *et al.* 2014, *MNRAS*, 438, 2701

https://doi.org/10.1017/S1743921315003336 Published online by Cambridge University Press